

## Establishment of subrenal capsule xenografts of primary human ovarian tumors in SCID mice: potential models

Cheng-Han Lee<sup>a,1</sup>, Hui Xue<sup>b,1</sup>, Margaret Sutcliffe<sup>b</sup>, Peter W. Gout<sup>b</sup>, David G. Huntsman<sup>a,c</sup>,  
Dianne M. Miller<sup>d</sup>, C. Blake Gilks<sup>a</sup>, Y.Z. Wang<sup>b,\*</sup>

<sup>a</sup>Department of Pathology, Genetic Pathology Evaluation Centre of the Prostate Centre, Vancouver General Hospital, BC Cancer Agency and University of British Columbia, Vancouver, BC, Canada V5Z 4E6

<sup>b</sup>Department of Cancer Endocrinology, BC Cancer Agency, Vancouver, BC, Canada V5Z 4E6

<sup>c</sup>Department of Pathology, BC Cancer Agency, Vancouver, BC, Canada V5Z 4E6

<sup>d</sup>Department of Gynecologic Oncology, BC Cancer Agency, Vancouver, BC, Canada V5Z 4E6

Received 21 July 2004

Available online 28 October 2004

### Abstract

**Objective.** To evaluate subrenal capsule xenografting of primary ovarian tumor tissues in mice for development of new ovarian cancer models.

**Methods.** Pieces (1 × 3 × 3 mm) of ovarian tumor specimens from patients were meticulously grafted under renal capsules of female NOD/SCID mice within 2 h of surgical removal. Tumor types included papillary serous adenocarcinomas, borderline and benign mucinous cystadenomas, granulosa cell tumors, a serous borderline tumor and a grade 3 mixed surface epithelial tumor of transitional and undifferentiated types. After 1–2 months, grafts were retrieved for comparison with original tissues. Hematoxylin and eosin (H&E) and immunohistochemical staining was carried out using tissue micro-arrays and CEA, B72.3, WT-1, OC125, keratin, inhibin, CK7, CK20, Cam5.2, and MIB-1 as markers.

**Results.** Tumor tissue engraftment rate was > 95%. Comparison of donor and post-graft tissues showed highly similar histopathological features; 91 ± 5% concordance in immunostaining indicated major preservation of immunophenotypes in the xenografts for 30–60 days. There was a small, but significant, increase in MIB-1 proliferative index in xenografts compared to original specimens.

**Conclusions.** Subrenal capsule xenografts of primary human ovarian tumors in SCID mice can retain major histopathological and immunohistochemical characteristics of the original tissues. The achievable, consistently high engraftment rate allows use of such xenografts as tools for studying a wide range of ovarian tumors, including granulosa cell tumors and benign, borderline, and malignant surface epithelial neoplasms. Potential applications include preclinical testing of patients' tumor responses to various chemotherapeutic regimens, evaluation of novel therapeutic agents, analysis of tumor progression at cellular and molecular levels, and identification of new therapeutic targets.

© 2004 Elsevier Inc. All rights reserved.

**Keywords:** Ovarian tumor tissue; In vivo; Renal capsule

### Introduction

Ovarian neoplasia encompasses a wide range of benign and malignant tumors, showing diversity in cell origin, biology, tumor grade, and extent of metastasis at presentation. In fact, as indicated by molecular genetic studies, ovarian cystadenomas, potential low malignant tumors, and carcinomas may not be part of a disease continuum, but represent separate disease entities [1]. In developing models

\* Corresponding author. Department of Cancer Endocrinology, BC Cancer Agency, 600 West 10th Avenue, Vancouver, BC, Canada V5Z 4E6. Fax: +1 604 877 6011.

E-mail address: [ywang@bccrc.ca](mailto:ywang@bccrc.ca) (Y.Z. Wang).

<sup>1</sup> Both authors contributed equally to this study.

for studying human ovarian neoplasia and creating new therapeutic modalities and diagnostic procedures, it is therefore of critical importance to ensure that the models closely resemble the various ovarian tumor types.

Many of the human ovarian cancer models reported are based on xenografts of established, but anaplastic, cancer cell lines in the subcutaneous compartment or peritoneal cavity of immunodeficient mice. While such models permit studies of cancer cell growth in an *in vivo* milieu, they generally do not accurately mimic the behavior of ovarian tumors in patients, nor do they properly predict the clinical efficacy of anticancer agents [2,3]. Various research groups have therefore attempted to establish more relevant models based on xenografts in immunodeficient mice of fresh, histologically intact human ovarian tumor tissues. Unfortunately, grafting of such tissues to the subcutaneous compartment [4], intraperitoneal cavity [5,6], or ovarian capsule, the orthotopic site [7], was found to be associated with low engraftment rates. Furthermore, xenografts could only be established using high-grade, advanced stage, but not low- or moderate-grade ovarian cancer tissues. A more promising site for grafting of ovarian tissue appeared to be the subrenal capsule location. Thus, grafting of cryopreserved normal human ovarian tissue under kidney capsules of immunodeficient mice allowed follicle maturation [8]. While the subrenal capsule site has been used for short-term drug sensitivity tests of human cancer tissue in immunocompetent mice (e.g., 6 days after grafting) [9–12], it has not been commonly used for xenografting of human cancer tissue in immunodeficient mice [13].

Recently, we have been able to improve engraftment rates for a variety of primary human tumor tissue xenografts in immunodeficient mice. Using tissues from cancers of the prostate, breast, colon, lung, kidney, and lymph nodes, we were able to achieve engraftment rates of >95% [14]. Technical refinements that contributed to the consistently high tumor take rate and viability of the xenografts include utilization of (i) the subrenal capsule grafting site, (ii) SCID mouse hosts, male or female, depending on the origin of the tumors, (iii) adjustment of the hormonal status of the host, if required, and (iv) surgical precision. In the present study, we have used this methodology for establishing xenografts of a range of benign and malignant primary ovarian tumors of surface epithelial and sex-cord stromal origin. The consistently high engraftment rate and major preservation of immunophenotypes in the xenografts indicate that such grafts provide potentially useful models for a variety of ovarian cancers.

## Materials and methods

### Materials and animals

Chemicals, stains, solvents, and solutions were obtained from Sigma-Aldrich Canada Ltd, Oakville, ON, Canada,

Table 1  
Patients' age, tumor histopathology and stage

Case VOA no.	Age of patient	Histopathology	Stage
160	59	Mucinous cystadenoma	NA
168	23	Borderline mucinous cystadenoma	1
162	36	Serous borderline tumor	1
151	41	Gr 1 serous cancer	3
150	53	Gr 3 serous cancer	3
158	75	Gr 3 serous cancer	3
163	53	Gr 3 serous cancer	3
167	71	Gr 3 serous cancer	2
161	75	Gr 3 transitional/undifferentiated cancer	2
152	70	Granulosa cell tumor	<sup>a</sup>
159	40	Granulosa cell tumor	1

NA: not applicable.

<sup>a</sup> Intra-abdominal recurrence of granulosa cell tumor.

unless otherwise indicated. Six- to eight-week-old female NOD/SCID mice were produced by the BC Cancer Research Centre Animal Resource Centre, BC Cancer Agency, Vancouver, Canada.

### Primary tumor tissue samples

Human ovarian tumor specimens were obtained at the Vancouver General Hospital (Vancouver, Canada) from 11 patients, with their informed consent, following a protocol approved by the Clinical Research Ethics Board of the University of British Columbia. The ages of the patients and histopathology of their tumors are presented in Table 1. The median age was 53 years (range 23–75 years). None of the patients had received treatment prior to tumor removal. There were five patients with papillary serous adenocarcinomas (one low grade and four high grade), one with borderline mucinous cystadenoma, one with benign mucinous cystadenoma, two with granulosa cell tumors, one with a serous borderline tumor and one with grade 3 mixed surface epithelial tumor of transitional and undifferentiated types. Six of the 10 patients with borderline or malignant ovarian tumors had advanced stage disease. Within 15 min of surgical removal, the tumor specimens were examined and sectioned by pathologists with parts selected for histological diagnosis, preservation in the National Ovarian Cancer Association Ovarian Tumor Bank (Vancouver, Canada), and subrenal capsule xenografting (see below).

### Subrenal capsule grafting procedure<sup>2</sup>

Using sterile conditions, an incision of approximately 2.0 cm is made along the midline of the skin in the back of an

<sup>2</sup> See <http://mammary.nih.gov/tools/Cunha001/index.html>.

anesthetized mouse. With the animal lying on its side, an incision is then made in the body wall slightly shorter than the long axis of a kidney. A kidney is slipped out of the body cavity by applying pressure on the other side of the organ using a forefinger and thumb. The exteriorized kidney is rested on the body wall and #5 fine forceps are used to gently pinch and lift the capsule from the parenchyma of the kidney to facilitate insertion of a 2–4-mm incision in the capsule using fine, spring-loaded scissors. A pocket between the kidney and the parenchyma is then created by blunt dissection. Care is taken not to damage the kidney parenchyma and thus prevent bleeding. The graft is transferred to the surface of the kidney using blunt-ended forceps. The cut edge of the kidney capsule is lifted with a pair of fine forceps and the graft is inserted into the pocket under the capsule using a polished glass pipette. Two or three grafts can be placed under the renal capsule with no apparent ill effect to the mouse. Once the grafting procedure has been completed, the kidney is gently eased back into the body cavity, the edges of the body wall and skin are aligned and closed with the aid of suture [15].

#### *Grafting of ovarian tumor tissue in SCID mice*

Tumor sections selected for grafting (pre-graft tissues) were stored at 4°C in Hanks' balanced salt solution supplemented with antibiotics. Within 2 h, each sample was cut into two parts. One part was fixed for histological analysis and the other was cut into multiple 1 × 3 × 3 mm pieces (2–24 pieces/specimen), which were meticulously grafted under renal capsules of 2–6 NOD/SCID mice (1–2/kidney). Xenografts (see Fig. 1) were retrieved after 30 or 60 days (post-graft tissues). If required, they were maintained by serial transplantation in SCID mice with transplant generations amounting to 30 or 60 days. Food and water were provided to the mice ad libitum; their health was monitored daily.

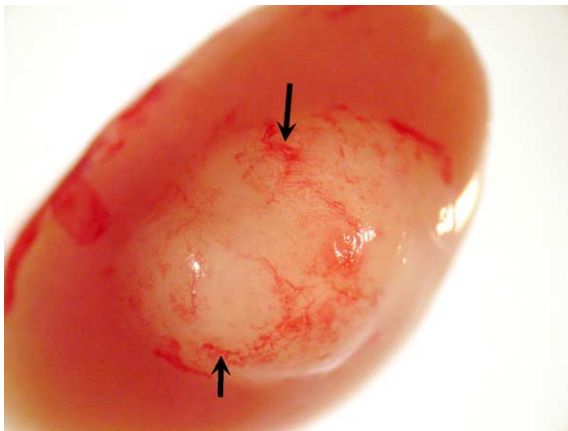


Fig. 1. Ovarian cancer tissue xenograft after 2 months of growth under the renal capsule of an intact female NOD/SCID mouse. Note the vascularization (arrows) of the graft.

Animal care and experiments were carried out in accordance with the guidelines of the Canadian Council on Animal Care.

#### *Construction of tissue microarrays*

Microscope slides carrying H&E-stained tissue sections showing representative tumor segments were selected and tumor areas marked. The corresponding formalin-fixed paraffin-embedded tissue blocks, from which the sections had been derived, were collected and the areas on the blocks, corresponding to the selected tumor areas on the slides, were circled with a felt pen for tissue micro array (TMA) construction. Using a Tissue Microarrayer (Beecher Instruments, Silver Spring, MD), two tissue cores from areas of interest in the donor blocks were removed with a 0.6-mm-diameter needle and inserted at high density into a single recipient paraffin block using a precise spacing pattern. Sections were cut from this TMA block with a standard microtome. In each case, the TMA sections included duplicate cores of donor, pre-graft, and post-graft tumor tissues.

#### *Immunohistochemical staining*

TMA sections were cut at a thickness of 4 µm on a microtome and mounted on glass microscope slides. For immunohistochemical staining, sections were de-waxed in Histoclear (National Diagnostic, Atlanta, GA) and hydrated in graded alcohol solutions and distilled water. Hematoxylin and eosin (H&E) staining was carried out as a routine, e.g., to monitor tumor viability. For immunophenotyping, antibodies were used against the following markers, depending on tissue availability, at the dilutions indicated: carcinoembryonic antigen (CEA)-p (Dako, Carpinteria, CA, 1:10,000); tumor-associated glycoprotein TAG-72 (B72.3) (ID Labs, London, Canada, 1:100); Wilms' tumor-1 (WT-1) (Dako, 1:50); ovarian cancer antigen CA125 (OC125) (ID Labs, 1:20); keratin (Dako, 1:4000); inhibin (Oxford BioInnovation, Oxfordshire, UK, 1:50); cytokeratin (CK) 20 (Dako, 1:500), CK7 (Dako, 1:200), and cytokeratin 8/18 (Cam5.2) (Becton-Dickinson, San Jose, CA, 1:50). The proliferation marker, Ki-67 nuclear antigen (MIB-1) (Immunotech, Marseilles, France, 1:100), was also used. Immunostaining was performed on 4-µm-thick tissue sections, using a Ventana automated immunostainer (Tuscon, AZ) according to the manufacturer's recommended procedures.

#### *Tissue microarray analysis*

After immunohistochemical staining, each TMA slide was scored by a pathologist (CBG). Tumor cell cytoplasmic or nuclear staining (as appropriate, according to the antigen being targeted) was scored as negative (<5% cells

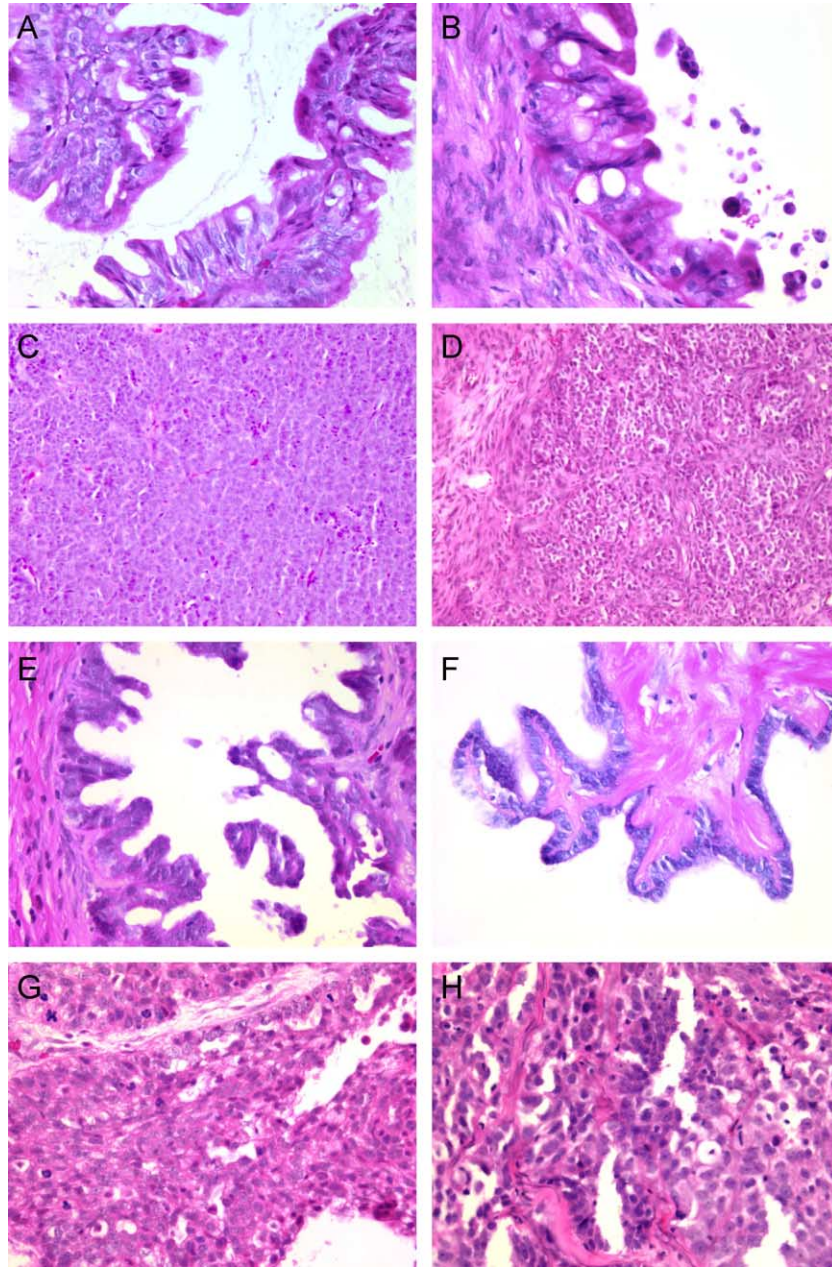


Fig. 2. Histopathology of representative donor and post-graft tumor tissues. H&E images of borderline mucinous cystadenoma donor (A) and post-graft (B) tumor tissues, granulosa cell tumor donor (C) and post-graft (D) tissues, serous borderline tumor donor (E) and post-graft (F) tissues, and a grade 3 serous carcinoma donor (G) and post graft (H) tissues.

positive, score of 0), weak positive (5–50% of cells showing weak or moderately intense positivity, score of 1), or strong positive (>50% of cells positive or 5–50% of cells showing intense staining, score of 2). For duplicate cores, score results were consolidated into one score/case where a higher score supersedes the lower score. Raw TMA staining data was processed by TMA-Deconvoluter software [16] into a format that allows for easy comparison. A difference in score of 1 or greater is considered a significant change in the immunophenotype. Concordance between duplicate cores scores was also analyzed to define

the intrinsic variability in immunostaining. For MIB-1-stained sections, the number of positively stained nuclei per 50 tumor cells in a randomly selected field was counted.

#### Statistical analysis

The Student's paired *t* test was used to check for differences in proliferation index between original donor and post-graft specimens. All average numerical results are shown as means  $\pm$  SEM. All statistical

Table 2  
Comparison of immunohistochemical phenotypes of donor and pre-graft tumor tissues

VOA no.	Histopathology	CEA-p	B72.3	WT-1	OC125	Keratin	Inhibin	CK20	CK7	Cam5.2
160	Mucinous cystadenoma	no Δ	no Δ		1→2	no Δ	no Δ	no Δ	no Δ	no Δ
168	Borderline mucinous cystadenoma	no Δ	no Δ	no Δ		no Δ	no Δ	no Δ	2→1	no Δ
162	Serous borderline tumor		no Δ		no Δ	no Δ			no Δ	no Δ
151	Gr 1 serous cancer	no Δ	no Δ	no Δ	no Δ	no Δ	no Δ	no Δ	no Δ	no Δ
158	Gr 3 serous cancer	no Δ	no Δ	no Δ	no Δ	1→2	no Δ	no Δ	no Δ	1→2
163	Gr 3 serous cancer	no Δ	no Δ	no Δ	no Δ	1→2	no Δ	no Δ	no Δ	1→2
167	Gr 3 serous cancer	no Δ	no Δ	no Δ		1→2	no Δ	no Δ	2→1	no Δ
161	Gr 3 transitional undifferentiated cancer	no Δ	no Δ	no Δ	1→2	no Δ	no Δ	no Δ	no Δ	no Δ

Note. “no Δ” means “no change”.

analyses were performed with SigmaPlot (SPSS Inc., US).

## Results

### *Establishment of xenografts from primary ovarian tumor tissues*

In all 11 cases, viable tumor tissue grafts were obtained under kidney capsules of female NOD/SCID mice, as indicated by H&E staining of sections (data not shown). Growth of the xenografts was slow, except for the grade 3 transitional/undifferentiated cancer that grew twice as much in volume within 15 days. No metastasis was observed in any of the hosts during the study period. Of a total of 108 tissue implantations, 104 were successful, resulting in an overall engraftment rate >95%.

### *Comparison of donor tissues and xenografts*

Histopathological comparisons of donor, pre-graft, and post-graft tumor tissues (see Materials and methods) were made for each patient's tumor specimen. In all cases, no major differences were observed among the three tissues with regard to architecture and cytological features. Representative H&E-stained tumor tissue sections are presented in Fig. 2.

In 8 of 11 cases, enough tumor tissue was available to allow immunophenotypic analysis using most of the immunomarkers. In the remaining three cases, only partial analysis could be performed. Comparisons of staining

intensities (obtained with the various markers) between donor and pre-graft tumor tissues and between donor and post-graft tumor tissues are presented in Tables 2 and 3, respectively. Absence of data reflects lack of tumor tissue. The results show that there were no substantial differences in staining intensities among the three groups. The minor differences found between donor and pre-graft tumor tissues likely reflect changes in the tumor tissue during its incubation in Hanks' balanced salt solution prior to grafting (up to 2 h), whereas the slight differences found between donor and post-graft tumor tissues reveal changes the tumor tissues underwent during the time spent in the hosts. As shown in Fig. 3, staining of borderline mucinous cystadenoma with Cam5.2, or of grade 3 serous carcinoma with WT-1 antibodies, showed similar staining intensity of donor and post-graft tissues. In general, strong staining was obtained for the low molecular weight keratin marker, Cam5.2, and weak staining for the WT-1 marker. While staining intensity with the various markers in general was similar for donor and post-graft tissues, CK7 staining intensity of one grade 3 transitional/undifferentiated cancer was lower for the post-graft tissue (Figs. 3E, F). The OC-125 staining localization and intensity between serous borderline tumor pre- (Fig. 3G) and post-graft (Fig. 3H) tissues was essentially identical. An overall comparison of the immunohistochemical phenotypes in donor, pre-graft, and post-graft tumor tissues revealed that the immunophenotype was well preserved through xenotransplantation, with an  $87 \pm 4\%$  overall concordance rate in immunostaining between donor and pre-graft tumor tissues and a  $91 \pm 5\%$  overall concordance rate in immunostaining between donor and post-graft tumor tissues. In a measure of

Table 3  
Comparison of immunohistochemical phenotypes of donor and post-graft tumor tissues

VOA no.	Histopathology	CEA-p	B72.3	WT-1	OC125	Keratin	Inhibin	CK20	CK7	Cam5.2
160	Mucinous cystadenoma	no Δ								
168	Borderline mucinous cystadenoma	no Δ								no Δ
162	Serous borderline tumor	no Δ	no Δ	no Δ	no Δ	no Δ	no Δ	no Δ	no Δ	no Δ
151	Gr 1 serous cancer	no Δ	no Δ	no Δ	no Δ	no Δ	no Δ	no Δ	no Δ	no Δ
158	Gr 3 serous cancer			no Δ		1→2			no Δ	
163	Gr 3 serous cancer	no Δ	no Δ	no Δ	no Δ	1→2	no Δ	no Δ	no Δ	1→2
167	Gr 3 serous cancer	no Δ	no Δ	no Δ		no Δ	no Δ	no Δ	no Δ	
161	Gr 3 transitional undifferentiated cancer	no Δ	no Δ	no Δ	no Δ	no Δ	no Δ	no Δ	2→1	

Note. “no Δ” means “no change”.

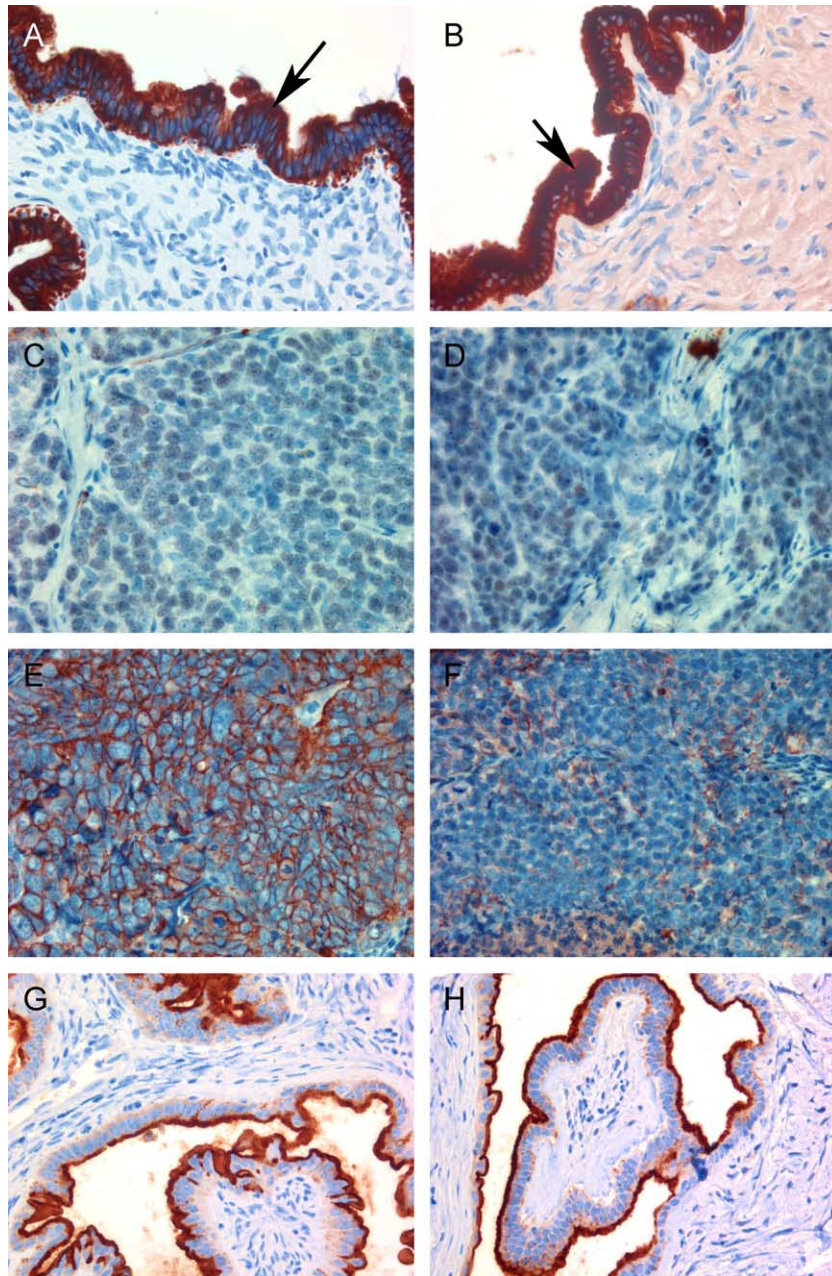


Fig. 3. Immunohistochemistry of representative donor and post-graft tumor tissues. Cam5.2 staining of borderline mucinous cystadenoma donor (A) and post-graft (B) tissues, with arrows pointing to stained epithelial cells; WT-1 staining of grade 3 serous carcinoma donor (C) and post-graft (D) tissues; CK7 staining of grade 3 transitional/undifferentiated cancer donor (E) and post-graft (F) tissues; OC-125 staining of serous borderline tumor pre- (G) and post-graft (H) tissues.

intratumoral heterogeneity of immunostaining, the concordance between duplicate cores taken either pre- or post-enucleation was  $90 \pm 5\%$ . The differences observed between the results obtained with the duplicate cores are not significant.

The proliferation indices of donor, pre-graft, and post-graft tumor tissues were assessed using MIB-1 immunostaining. All samples from individual tumors showed comparable values (Table 4). Overall, there was a  $6.5 \pm 2.3\%$  increase in the MIB-1 proliferative index in post-graft

tumor tissues as compared to the original tissues ( $P = 0.02$ , Student's paired  $t$  test).

## Discussion

There is accumulating evidence that the tissue environment of tumor cells plays a critical role in their growth and malignant progression. Thus, while stroma surrounding epithelia can act as a source of oxygen, nutrients, and

Table 4  
Tumor type and MIB-1 proliferative indices of donor, pre-graft, and post-graft tumor tissues

VOA no.	Tumor type	Donor tissue <sup>a</sup>	Pre-graft tissue <sup>a</sup>	Post-graft tissue <sup>a</sup>
160	Mucinous cystadenoma	0	0	
168	Borderline mucinous cystadenoma	5	11	6
162	Serous borderline tumor	0	1	1
151	Gr 1 serous cancer	5	7	4
150	Gr 3 serous cancer	10	13	13
158	Gr 3 serous cancer	10	12	10
163	Gr 3 serous cancer	14	15	20
167	Gr 3 serous cancer	19	17	25
161	Gr 3 transitional undifferentiated cancer	32	40	43
152	Granulosa cell tumor	5	7	8
159	Granulosa cell tumor	2	3	4

<sup>a</sup> Number of stained nuclei per 50 tumor cells.

growth stimuli, there are strong indications that it also has a stimulatory and regulatory function in the development of epithelial tumors [17,18]. In constructing xenograft tumor models that closely resemble human ovarian neoplasia, it appears therefore imperative to utilize tumor specimens that do not only contain tumor cells (including tumor subpopulations), but also tumor-associated stroma. In the present study, we achieved a consistently high engraftment rate (>95%) for tissue of primary human ovarian tumors grafted under the kidney capsules of female SCID mice. The tumors included granulosa cell tumors and benign, borderline, and malignant surface epithelial neoplasms. Of the surface epithelial tumors, one benign, two borderline, one low-grade malignant and five high-grade malignant cases were studied. This encompasses the full spectrum of ovarian surface epithelial tumor pathology. Upon grafting, the tumor tissues largely retained their histological and immunophenotypic characteristics as evaluated with up to nine immunomarkers; they also showed stable proliferative indices as assessed with MIB-1 staining. Whenever there was a change in the immunostaining score, it was relatively small, never exceeding 1 unit. Similar differences in immunostaining were observed when duplicate cores from a single sample were compared, indicating that the minor changes observed can be accounted for by intratumoral staining variability and are not related to the xenograft procedure. Taken together, the results indicate that the subrenal capsule xenografting procedure can lead to preservation, under in vivo conditions, of tumor tissue without loss of its major tissue characteristics.

It has recently been suggested that low-grade and high-grade serous carcinomas arise via different molecular pathways [19,20]. In the present study, xenografts were successfully obtained from both grade 1 and grade 3 serous carcinomas without major changes in nine different immunophenotypic properties or proliferative indices (Tables 2–4). It appears therefore that the mechanisms involved in the development of such malignancies can

now be studied in a relevant in vivo model. Similarly, subrenal capsule xenografts of granulosa cell tumors and mucinous cystadenomas in SCID mice should allow greater in-depth studies concerning optimal therapy and identification of molecular and cellular events during oncogenesis.

In conclusion, the present study has demonstrated that the subrenal capsule site in SCID mice can be successfully used for grafting of a wide variety of primary human ovarian tumors, including granulosa cell tumors and benign, borderline, and malignant surface epithelial neoplasms. The consistently high engraftment rate and major preservation of immunophenotypes obtained indicate that such xenografts can be used as tools in studies aimed at a better understanding of ovarian tumorigenesis. Potential applications of the xenografts include preclinical testing of patients' tumor responses to various chemotherapeutic regimens, evaluation of novel therapeutic agents and diagnostic methods, analysis of tumor progression at cellular and molecular levels, and identification of new therapeutic targets.

## Acknowledgments

The authors thank Yuwei Wang and Rebecca Wu for excellent technical assistance.

This work was supported in part by NCI Canada grant no. 014053 and funding from OvCaRe, an initiative of the VGH and UBC Hospital Foundation and the BC Cancer Foundation, Vancouver, Canada (Y.Z.W.), a grant from the National Ovarian Cancer Association, Canada (C.B.G.), and an educational grant from Aventis Pharma Inc. (D.G.H.). Dr. David G. Huntsman is a Michael Smith Foundation for Health Research Scholar.

## References

- [1] McCluskey LL, Dubeau L. Biology of ovarian cancer. *Curr Opin Oncol* 1997;9(5):465–70.
- [2] Buick RN, Pullano R, Trent JM. Comparative properties of five human ovarian adenocarcinoma cell lines. *Cancer Res* 1985;45(8):3668–76.
- [3] Boven E, Nauta MM, Schluper HM, Erkelens CA, Pinedo HM. Superior efficacy of trimelamol to hexamethylmelamine in human ovarian cancer xenografts. *Cancer Chemother Pharmacol* 1986;18(2):124–8.
- [4] Verschraegen CF, Hu W, Du Y, Mendoza J, Early J, Deavers M, et al. Establishment and characterization of cancer cell cultures and xenografts derived from primary or metastatic Mullerian cancers. *Clin Cancer Res* 2003;9(2):845–52.
- [5] Schumacher U, Adam E, Horny HP, Dietl J. Transplantation of a human ovarian cystadenocarcinoma into severe combined immunodeficient (SCID) mice-formation of metastases without significant alteration of the tumour cell phenotype. *Int J Exp Pathol* 1996;77(5):219–27.
- [6] Elkas JC, Baldwin RL, Pegram M, Tseng Y, Slamon D, Karlan BY. A

- human ovarian carcinoma murine xenograft model useful for preclinical trials. *Gynecol Oncol* 2002;87(2):200–6.
- [7] Kiguchi K, Kubota T, Aoki D, Udagawa Y, Yamanouchi S, Saga M, et al. A patient-like orthotopic implantation nude mouse model of highly metastatic human ovarian cancer. *Clin Exp Metastasis* 1998;16(8):751–6.
- [8] Aubard Y. Ovarian tissue xenografting. *Eur J Obstet Gynecol Reprod Biol* 2003;108(1):14–8.
- [9] Bogden AE, Haskell PM, LePage DJ, Kelton DE, Cobb WR, Esber HJ. Growth of human tumor xenografts implanted under the renal capsule of normal immunocompetent mice. *Exp Cell Biol* 1979;47(4):281–93.
- [10] Bogden AE, Cobb WR, Lepage DJ, Haskell PM, Gulkin TA, Ward A, et al. Chemotherapy responsiveness of human tumors as first transplant generation xenografts in the normal mouse: six-day subrenal capsule assay. *Cancer* 1981;48(1):10–20.
- [11] Griffin TW, Bogden AE, Reich SD, Antonelli D, Hunter RE, Ward A, et al. Initial clinical trials of the subrenal capsule assay as a predictor of tumor response to chemotherapy. *Cancer* 1983;52(12):2185–92.
- [12] Stratton JA, Kucera PR, Rettenmaier MA, Dobashi K, Micha JP, Braly PS, et al. Accurate laboratory predictions of the clinical response of patients with advanced ovarian cancer to treatment with cyclophosphamide, doxorubicin, and cisplatin. *Gynecol Oncol* 1986;25(3):302–10.
- [13] Kleine W. In vivo chemosensitivity test models for gynecologic malignancies: methodology and results. In: Kochli OR, Sevin BU, Haller U, editors. *Chemosensitivity testing in gynecologic malignancies and breast cancer*. Basel: Karger, 1994. p. 76–81.
- [14] Wang YZ, Sudilovsky D, Cao M, Chen W, Goetz L, Xue H, et al. Establishing efficient xenograft models of low-grade human prostate cancer. *Eur Urol, Suppl* 2003;2(6):30.
- [15] Wang YZ, Sudilovsky D, Zhang B, Haughney PC, Rosen MA, Wu DS, et al. A human prostatic epithelial model of hormonal carcinogenesis. *Cancer Res* 2001;61(16):6064–72.
- [16] Liu CL, Prapong W, Natkunam Y, Alizadeh A, Montgomery K, Gilks CB, et al. Software tools for high-throughput analysis and archiving of immunohistochemistry staining data obtained with tissue microarrays. *Am J Pathol* 2002;161(5):1557–65.
- [17] Pupa SM, Menard S, Forti S, Tagliabue E. New insights into the role of extracellular matrix during tumor onset and progression. *J Cell Physiol* 2002;192(3):259–67.
- [18] Kenny PA, Bissell MJ. Tumor reversion: correction of malignant behavior by microenvironmental cues. *Int J Cancer* 2003;107(5):688–95.
- [19] Singer G, Oldt III R, Cohen Y, Wang BG, Sidransky D, Kurman RJ, et al. Mutations in BRAF and KRAS characterize the development of low-grade ovarian serous carcinoma. *J Natl Cancer Inst* 2003;95(6):484–6.
- [20] Singer G, Shih Ie M, Truskinovsky A, Umudum H. Mutational analysis of K-ras segregated ovarian serous carcinomas into two types: invasive MPSC (low-grade tumor) and conventional serous carcinoma (high-grade tumor). *Int J Gynecol Pathol* 2003;22:37–41.